Thermochimica Acta, 222 (1993) 241–253
Elsevier Science Publishers B.V., Amsterdam

IR and UV spectral and differential thermal analyses of symmetry shifts in geminally bis-, tetrakis- and fully substituted phenyl derivatives of cyclotriphosphazene

Abdulla H. Al-Kubaisi and Moein B. Sayed *
Chemistry Department, Qatar University, Doha-2713 (Qatar)

(Received 23 November 1992; accepted 14 December 1992)

Abstract

The effect of geminal arylation on the hexachlorocyclotriphosphazatriene molecular structure and on the thermodynamics has been investigated by infrared and ultraviolet spectroscopy and by differential thermal analysis. The spectral and thermal evidence suggest that D_{3h} is the point group to which the molecular symmetry of this compound should be referred. Arylation to both the bisphenyl and tetrakisphenyl derivatives reduces the molecular symmetry to the C_{2v} point group, which influences the spectral and thermal features dramatically. Further arylation to the hexaphenyl derivative raises the symmetry to puckered C_{3v}, which undergoes a thermal shift into the higher D_{3h} point group. Except for the hexaphenyl derivative, all the studied phosphazenes show only a solid–liquid phase transition. The hexaphenyl derivative shows an additional solid–solid phase transition, which can probably be attributed to the proposed solid state C_{3v}–D_{3h} point-group symmetry transfer. Protonation of the phenyl phosphazenes is expected to proceed symmetrically at the three nitrogen atoms of the ring, because the molecular symmetry is maintained, as shown by the unshifted spectral features. However, the protonation process shifts the molecular structure into a more associative, rigid solid phase, which influences the spectral and thermal features and provides a broader, more diffused structure.

INTRODUCTION

Phosphazenes have been classified [1] into three major categories according to the coordination number of the phosphorus: (i) two-coordinate tervalent phosphorus [2], (ii) three-coordinate quinquevalent phosphorus [3], and (iii) four-coordinate quinquevalent phosphorus [4, 5]. Among the second category of compounds, long-range cyclotriphosphazatrienes $N_3P_3X_6$ (where X is an element or group of elements) have been of special interest because of their activity to numerous chemical reactions, unique bonding scheme, peculiar structural and spectral features, and various important applications in both practical and industrial problems.

* Corresponding author.

The aziridine derivatives $N_3P_3Az_6$ have been used as anti-cancer drugs and insect chemosterilants [6–10]. Because they incorporate P and N atoms, cyclotriphosphazatrienes have excellent applications as both fertilizers [11–13] and fire extinguishers [14–16]. Because of the potential importance of these compounds, their chemistry has been extensively studied and reviewed [17–20].

Hexachlorocyclotriphosphazatriene is a noteworthy derivative, as it is considered as a key route to the synthesis of the majority of the other derivatives. It was first identified by Liebig and Wohler [21] and was prepared by ammonolysis of phosphorus pentachloride with ammonium chloride [22–24]. The phenyl-substituted derivatives have been prepared via various routes of ring closure [25–27], the well established Friedel–Crafts [27–29] reaction of the chloro-derivative with benzene and Grignard synthesis [30]. The Friedel–Crafts reaction yields geminally substituted derivatives, because ≡PClph is a more reactive centre than $\equiv PCl_2$ [31], whereas synthesis using a Grignard reagent leads to low-yield phenyl derivatives.

The hexachloro derivative, as well as many other symmetrically substituted derivatives, has D_{3h} symmetry. However, in the solid state, these compounds might undergo a symmetry shift into a slightly puckered ring structure of C_{3v} symmetry [32, 33], in which both the chair [34] and boat [35] conformations could be resolved. Nevertheless, the D_{3h} symmetry becomes increasingly dominant in the more flexible molten and solution states [36–38].

The symmetry and structure shifts, observed upon arylation and protonation of the titled compounds, should induce both spectral and thermal shifts, which can be followed by structure-probe infrared (IR) and ultraviolet–visible (UV) spectroscopy and by differential thermal analysis (DTA). The structural interpretation of the DTA data is presented here for the compounds under consideration.

EXPERIMENTAL

Materials and procedure

The materials used were hexachlorocyclotriphosphazatriene (Nippon Soda Co. Ltd.), dry benzene (BDH), anhydrous aluminium chloride (Fluka) and triethylamine (Riedel-de Haen).

Friedel–Crafts arylation of cyclotriphosphazatriene was applied stoichiometrically to the syntheses of the geminally substituted bis and tetrakis derivatives. Synthesis of the fully substituted phenyl derivative was necessarily performed in an excess of benzene, with the aid of an HCl-abstracting agent, e.g. triethylamine. Because HCl is one of the

TABLE 1

The thermodynamic features of the phosphazene compounds

Derivative	Phase transition	Symbol [a]	T_c/K	$E^{\#}$/ kJ g^{-1} K^{-1}	ΔH/ J g^{-1}	ΔS/ g^{-1} K^{-1}	α
Hexachloro	Solid–liquid I	○	388	550	13.782	0.036	0.16
Bisphenyl	Solid–liquid II_a	□	369	545	11.387	0.031	0.29
Protonated bis-	Solid–liquid II_b	■	340	261	2.714	0.008	0.07
Protonated tetrakis-	Solid–liquid III	△	413	146	3.300	0.008	0.04
Protonated hexa-	Solid–liquid IV_b	◇	510	602	8.620	0.017	0.04
Protonated hexa-	Solid–solid IV_a	◆	438	220	7.450	0.017	0.04

[a] Refers to the figures.

reaction products, protonation of the ring nitrogens is increasingly possible for the more mesomeric substituted phenyl derivative. This facilitated a study of the effect of ring protonation as well as that of increased molecular mesomerism on the phosphazene structure and thermodynamics. Following this method of arylation, the phenyl derivatives of Table 1 were successfully separated into a pure phase [27, 38, 39] and were identified by their elemental analysis and melting points; their structural features were characterized both spectrally by IR and UV spectroscopy and thermally by DTA.

Equipment

The IR measurements were performed in the solid state, using the KBr disc technique and a Nicolet FT-IR 510P spectrometer. UV measurements were performed in 10^{-3} M ethanol solution, using a Beckman DU70 spectrophotometer. The DTA of these compounds was performed in air for samples weighing 30 mg, using a Shimadzu DSC TA 30 thermal analyser in the temperature range 273–673 K range, with a temperature rise of 10 K min^{-1}. The thermal data were computer-processed, and treated as described elsewhere [40].

RESULTS AND DISCUSSION

Spectral analysis

Infrared spectra

In the 4000–2400 cm^{-1} spectral region, the IR spectrum of the hexachloro derivative (Fig. 1, curve I) shows no measurable absorptions. The geminally bisphenyl derivative shows a triplet band (Fig. 1, curve IIa) at 3058 cm^{-1} typical of the mono-substituted benzene Ar–H stretching mode. Protonation of this derivative induces two spectral shifts (Fig. 1,

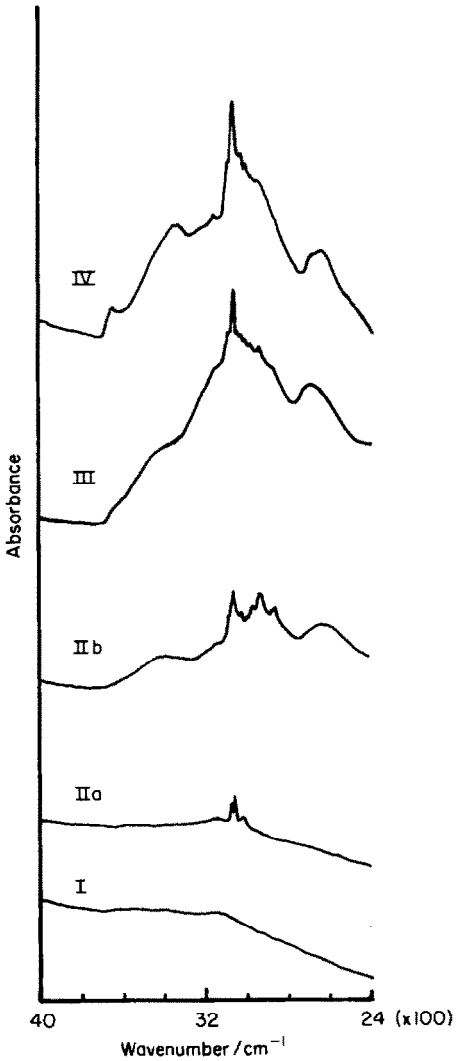

Fig. 1. Solid state infrared (4000–2400 cm^{-1}) spectra of the phosphazene derivatives in the spectral range of the Ar–H and N–H stretching modes. For an identification of the curves, see Table 1.

curve IIb): an enhanced absorbance and the appearance of a new triplet band at 2924 cm^{-1}. Both shifts can be attributed to a proton-induced bond polarization of the Ar–H bonds. Evidence of this ring protonation is explicit in the appearance of characteristic N^+–H bands at 3370 and 2620 cm^{-1} for the stretching modes, and at lower frequencies (see below) for the deformation modes. The progressive rise in the band absorbance of these features (Fig. 1, curves III and IV) reflects the corresponding increase in the phenyl increment.

In the more descriptive 2000–200 cm^{-1} region, the IR spectrum of the

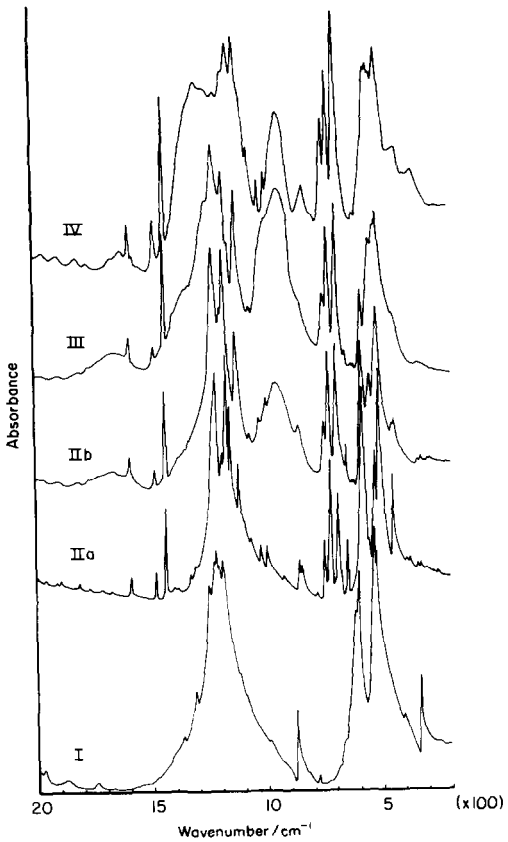

Fig. 2. Solid state infrared (2000–200 cm^{-1}) spectra of the phosphazene derivatives in the fingerprint spectral range. For an identification of the curves, see Table 1.

hexachloro derivative (Fig. 2, curve I) is dominated by three split bands at 1221, 603 and 529 cm^{-1}. The first band is attributed to the phosphazene ring-breathing mode, which incorporates other less important combination and Fermi-resonance bands at both the higher and lower frequency sides. The 603 and 529 cm^{-1} bands are assigned to the asymmetric and symmetric stretching modes of PCl_2, respectively. The split appearance of these modes is a consequence of the solid-state-induced puckered ring structure [41–44], which slightly modifies the D_{3h} point group of symmetrically substituted phosphazenes into the less symmetric C_{3v} point group. Nevertheless, the fairly simple spectrum suggests that D_{3h} is the dominant point group. The less dominant bands at 874 and 332 cm^{-1} may be assigned to other less probable P–N ring vibrations.

Geminal substitution into the bisphenyl derivative is presumed to reduce the molecular symmetry further to the C_{2v} point group. This complicates the spectrum (Fig. 2, curve IIa) with the substituent's vibrations as well as with other IR-activated modes. Regarding the newly incorporated modes,

the bands at 1591 and 1483 cm^{-1} are typical of mono-substituted phenyl ring-breathing modes. The sharp band at 1439 cm^{-1} may be assigned to P–Ar or to other phenyl-ring-activated modes. Assignment to the latter species seems more plausible, because geminal PAr_2 would yield asymmetric and symmetric modes rather than a single mode. The PAr_2 stretching modes appear at the rather lower frequencies of 529 and 507 cm^{-1}. Also, the 1028 and 1000 cm^{-1} bands are typical of mono-substituted phenyl ring vibrations. The aromatic Ar–H deformations at 1121 cm^{-1} (in-plane) and 748, 723 and 690 cm^{-1} (out-of-plane) are also typical of mono-substituted benzene derivatives. However, the phosphazene 1221 cm^{-1} vibration shows a greater splitting of 48 cm^{-1} for the bisphenyl derivative, as compared to 30 cm^{-1} in the hexachloro derivative, which agrees with the proposed geminal substitution for the more bulky phenyl groups [20]. Also, the P–N modes at 874 and 332 cm^{-1} show considerable splitting. However, the splitting of the PCl_2 modes merges and its bands shift to lower frequencies at 583 and 449 cm^{-1}, respectively. The downward shift in these modes is a result of increased molecular mesomerism, whereas the merged splitting indicates a symmetric location of the four chlorine atoms.

In addition to these spectral data, broad bands typical of the N^+–H in-plane and out-of-plane bending modes appear for the protonated derivative (Fig. 2, curve IIb) at 1665 and 955 cm^{-1}, which is considered complementary to the higher frequency 4000–2400 cm^{-1} spectral data. At variance with the other vibrational modes, the P–N mode at 874 cm^{-1} is selectively sensitive to the protonation, where it shows a considerable downward shift to 828 cm^{-1}. It is important to note that protonation of the phosphazene ring must take place equally at the three ring nitrogens, because the molecular symmetry is not shifted, as can be observed (Fig. 2, curves IIa and IIb) in the unchanged spectral patterns.

The spectrum of the tetrakisphenyl derivative (Fig. 2, curve III) shows no shifts in the band frequencies when compared with the spectrum of the bisphenyl derivative, because both have the same C_{2v} point group. Nevertheless, significant arylation-induced shifts in the band absorbance of both the PAr_2 and PCl_2 modes can be clearly observed. While the PCl_2 band absorbance at 583 and 449 cm^{-1} is reduced, that of PAr_2 at 529 and 507 cm^{-1} rises. A corresponding rise in the absorbance of the phenyl ring and Ar–H bond vibrations is also observed, which is consistent with the increase in the phenyl increment.

The spectrum of the hexaphenyl derivative (Fig. 2, curve IV) confirms the conclusions derived from spectrum III. While the PCl_2 bands vanish entirely, those of phenyl and PAr_2 attain their maximum absorbance. Moreover, the phosphazene ring-breathing mode at 1221 cm^{-1} shifts upward to 1294 cm^{-1}, which agrees with the mesomerism-induced rise in the P–N bond order, and therefore, band frequency. A similar effect of the increased mesomeric structure is also evident in UV spectroscopy.

The assignments made here are based on spectral correlations with comparable literature data [45, 46].

Ultraviolet spectra

The hexachloro derivative (Fig. 3, curve I) shows a low absorption coefficient at 204 nm typical of the phosphazene $\pi \rightarrow \pi^*$ transition [47], which is the direct result of a totally symmetric, low-dipole ring structure; this confirms the D_{3h} point group assignment, rather than the puckered C_{3v} symmetry. This transition shifts with the arylation (Fig. 3, curve II), to both a higher coefficient and a longer wavelength band at 230 nm; both shifts illustrate the effect of increased mesomerism on the molecular structure. The low absorption coefficient of the phenyl $\pi \rightarrow \pi^*$ transition at 264 nm could be associated with its low dipole, as compared with that of the arylation-enhanced phosphazene transition.

Further substitution with phenyl rings, however, does not significantly

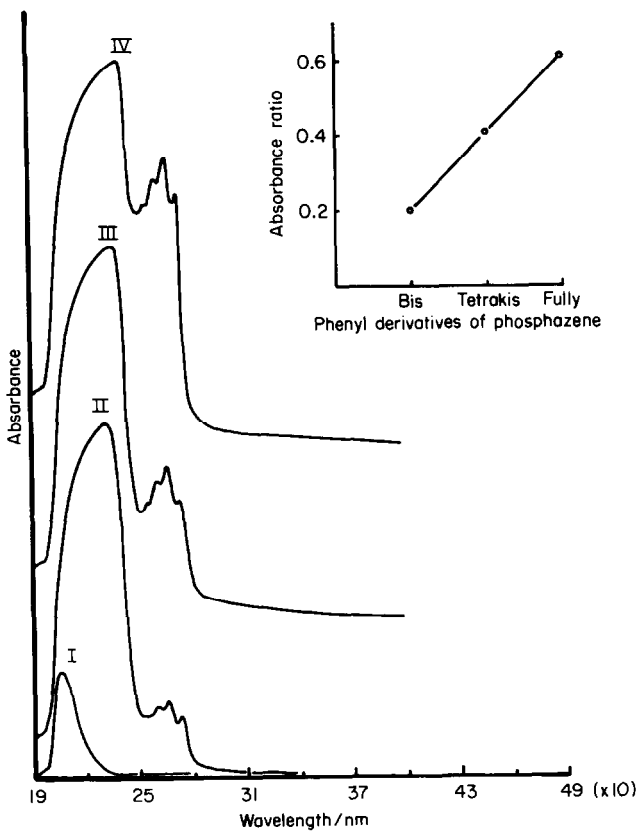

Fig. 3. Solution ultraviolet (190–490 nm) spectra of the phosphazene derivatives in 10^{-3} M ethanol. The inset illustrates the dependence of the phenyl/phosphazene absorbance ratio on the phenyl content of the phosphazene. To identify the curves, see Table 1.

affect the phosphazene transition, except for a slight upward shift to longer wavelengths of 234 and 240 nm for the tetrakisphenyl and hexaphenyl derivatives, respectively, the band absorbance of the phenyl transition being progressively increased [48]. The well observed increase in absorbance, rather in the absorption coefficient, is associated with a corresponding rise in the phenyl content of the phosphazene (Fig. 3, inset).

So far, the IR and UV spectral analyses have demonstrated how the molecular structure of phosphazene changes upon Friedel–Crafts arylation. This structural information provides the basis for the discussion of the thermal features and thermodynamic shifts observed with phenyl substitution.

Thermal analysis

The DTA thermograms of the phosphazenes under investigation show endothermic solid–solid and solid–liquid phase transitions which depend on the molecular symmetry, as well as other less significant exothermic transitions of the decomposition products which take place above 600 K. Only the former endothermic transitions are of interest, as they illustrate the effect of structural shifts on the thermodynamics of the compounds.

The solid–liquid phase transition of both the free hexachloro and bisphenyl derivatives is characterized by a fairly sharp peak, as compared to the much broader peak shown by the protonated derivatives. The broad band structure, whether thermal or spectral, of the protonated phosphazenes indicates the highly associated states of these compounds.

The specific heat C_p (Fig. 4) provides a measure of these broadly qualitative thermal data. Arylation into the bisphenyl derivative reduces the T_c and C_p of the solid–liquid transition of the hexachloro derivative (Fig. 4, curve I) to a less thermally stable solid (Fig. 4, curve IIa and Table 1). This is the direct result of the arylation-enhanced molecular mesomerism evident from IR and UV spectroscopy. Protonation of the resultant bis derivative also appears to assist the reduction of these thermal features (Fig. 4, curve IIb and Table 1). This is rather surprising, because HCl–salt formation is known generally to assist the thermal stability of the solid-state. The symmetric protonation of the phosphazene ring appears to be the reason for the lowered C_p and T_c. The presence of a symmetrically distributed positive charge in conjugation with the phosphazene ring delocalized electrons assists the molecular mesomerism. Evidence of this is depicted in the highly polarized Ar–H bonds, as revealed by IR spectroscopy.

Further arylation into the protonated tetrakisphenyl and hexaphenyl derivatives enhances the broad band structure (Fig. 4, curves III and IVb), indicating proton-enhanced associated phases. This assists in raising the T_c (Table 1) of the solid–liquid transition of these derivatives.

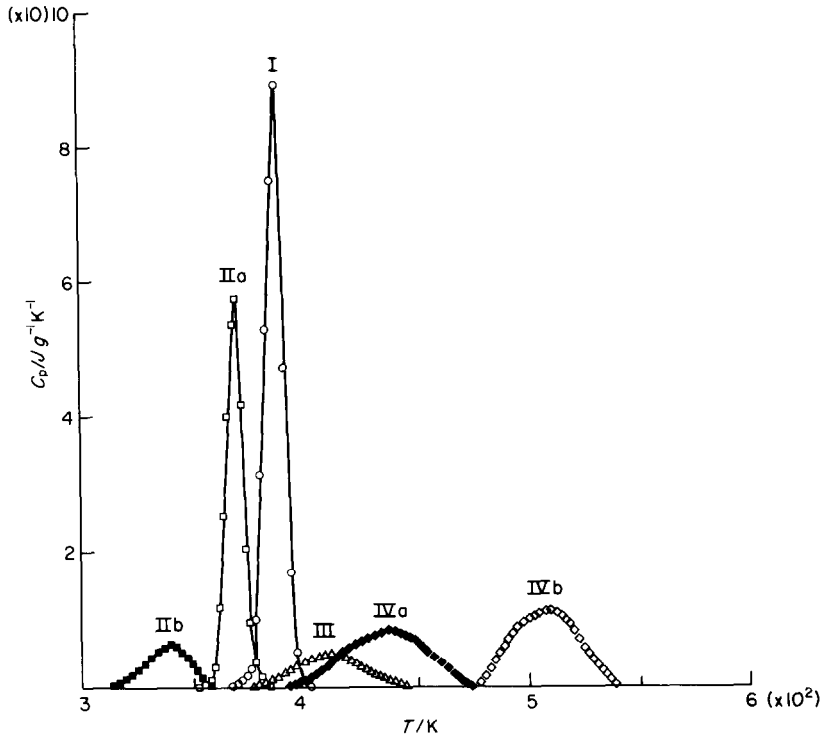

Fig. 4. Specific heat C_p of the solid–solid and solid–liquid phase transitions of the phosphazenes. To identify the curves, see Table 1.

It is very interesting to observe that while all the studied compounds show a solid–liquid phase transition, only the hexaphenyl derivative has an additional solid–solid phase transition (Fig. 4, curve IVa), where the phosphazene crystals swell and shine brightly, indicating internal motion on a molecular scale. This could be where the hexaphenyl derivative rearranges its molecular structure from the puckered C_{3v} into the higher D_{3h} symmetry, in agreement with the previously published findings. Because such a solid state phase transition is not quoted for the hexachloro derivative, and because of both its very simple IR spectrum and the totally symmetric, low-dipole UV $\pi \rightarrow \pi^*$ transition, it can be concluded that the hexachloro derivative shows totally symmetric D_{3h} symmetry, rather than the C_{3v} point group.

The enthalpy change of the transition ΔH was calculated using the peak area method, with reference to a pure indium ΔH of 28.4 J g^{-1} measured at 703 K. The values calculated (Table 1) are higher for the non-associated hexachloro and bisphenyl phosphazenes. The close, small ΔH values of the protonated bisphenyl and tetrakisphenyl derivatives suggests that the low thermal stability of these derivatives reflects their low molecular symmetry. Thus, raising the molecular symmetry from C_{2v} point group to solid-state

C_{3v} and further to the more thermally stable D_{3h} point group of hexaphenyl derivative, increases the ΔH values (Table 1).

Calculation of the transition entropy change ΔS would further clarify the connection between the molecular symmetry and the thermodynamics of these compounds. It is not surprising that the ΔS values for the solid–solid and solid–liquid transitions of the hexaphenyl derivative are the same, because they belong to the same molecular species. Likewise, the ΔS values for the solid–liquid transitions of the bisphenyl and tetrakisphenyl derivatives reflect the same C_{2v} point group. The higher ΔS of the hexaphenyl derivative can be attributed to its higher molecular symmetry. It is important to stress that it is inappropriate to correlate the ΔS data of the non-protonated and protonated species in this respect.

The transition activation energy $E^{\#}$ can be estimated by plotting the logarithmic form of the equation

$$C_p = (ZNE^{\#2}/RT^2)e^{-E^{\#}/RT} \quad (1)$$

where Z is the coordination number, N the number of defects, R the universal gas constant and $E^{\#}$ the transition activation energy, see Fig. 5.

The slope of the linear dependence, particularly far from T_c (Fig. 5), is

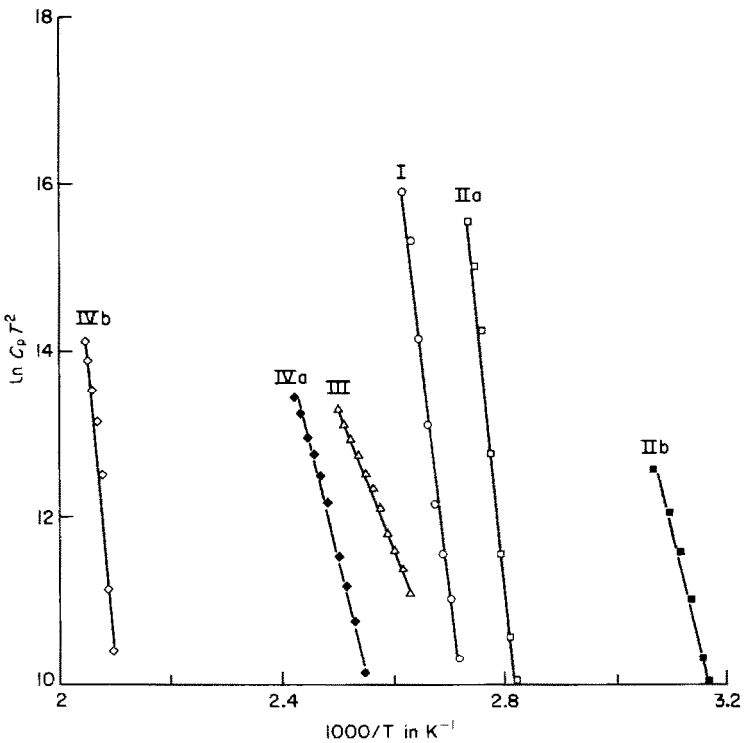

Fig. 5. Dependence of the transition C_p on $1/T$ as a measure of the transition activation energy. To identify the curves, see Table 1.

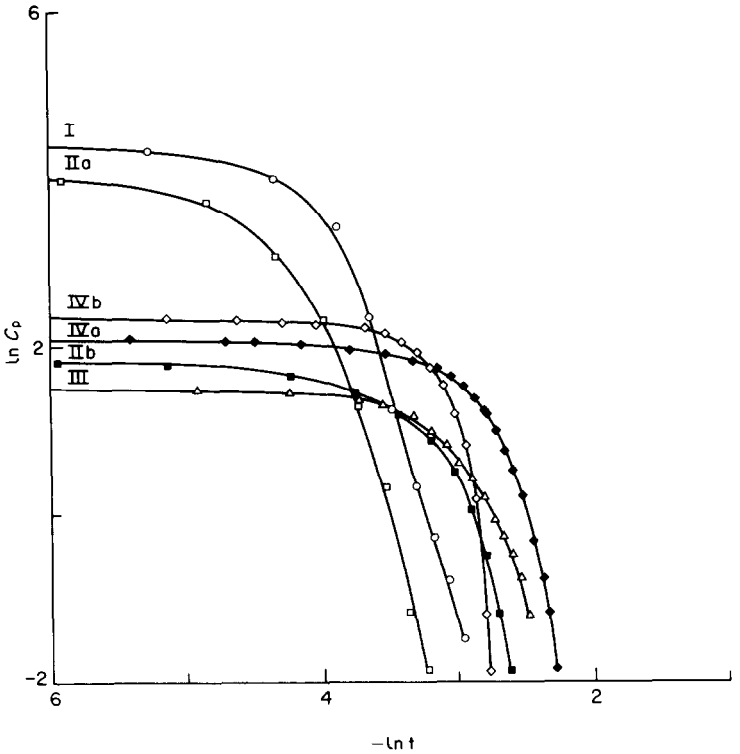

Fig. 6. Dependence of the transition C_p on the temperature shift t as a measure of the thermodynamic transition model. To identify the curves, see Table 1.

considered a measure of the activation energy. The calculated values are reported in Table 1. The totally symmetric hexaphenyl and hexachloro phosphazene derivatives are distinguished by the highest activation energy. The lowest energy is reported for the tetrakisphenyl derivative, which seems to display only slight arylation-enhanced mesomerism and protonation-induced association; their opposing effects seem to cancel out in this compound.

Finally, it is interesting to determine which model best describes the phase transitions of these compounds. The thermodynamic structural model α can be calculated [49] from the logarithmic dependence of the equation

$$C_p = At^{-\alpha} \tag{2}$$

where A is a constant and t equals $(T - T_c)/T_c$. The values obtained for the protonated phosphazenes are fairly compatible with the 3-dimensional Ising model [50]. The higher values obtained for the free hexachloro and bisphenyl derivatives, although still in the range for the Ising model, may reflect a disordered random distribution [51], which is also indicated in their higher entropy changes, see Table 1 and Fig. 6.

ACKNOWLEDGEMENTS

The authors express their great thanks to Dr. Sharifa El-Kaabi of the Chemistry Department and Dr. Gabr El-Neimi of SARC, Qatar University for their kind cooperation in using the UV and IR spectrometers.

REFERENCES

1 R.A. Shaw, Phosphorus and Sulphur, 4 (1978) 101.
2 D.E.C. Corbridge, The Structural Chemistry of Phosphorus, Elsevier, Amsterdam, 1974, p. 272.
3 E. Nieke and O.J. Schere, Nachr. Chem. Tech., 23 (1975) 395.
4 E. Nieke and W. Flick, Angew. Chem. Int. Ed. Engl., 12 (1973) 585.
5 O.J. Schere and N. Kuhn, Chem. Ber., 107 (1974) 2123.
6 O.C. Dermer and G.E. Ham, Ethyleneimine and Other Aziridine Chemistry and Applications, Academic Press, New York, 1969.
7 R.W. Allen, J.P. O'Brien and H.R. Allcock, J. Am. Chem. Soc., 99 (1977) 3987.
8 J.F. Labarre, J.P. Faucher, L. Gaston, F. Sourines, S. Cros and G. Francois, Eur. J. Cancer, 15 (1979) 637.
9 J.P. Faucher, F. Cragnier and J.F. Labarre, J. Mol. Struct., 26 (1981) 165.
10 J.F. Labarre, Top. Curr. Chem., 102 (1982) 1.
11 A.P. Conesa, C. R. Seances Acad. Agric. Fr., 60 (1974) 1353.
12 W. Wanek, Pure Appl. Chem., 44 (1975) 459.
13 S.S. Krishnamurthy, R.A. Shaw and M. Woods, Current Sci., 45 (1976) 433.
14 C.V. Stevens and S.W. Sello, Proc. Symp. Text. Flammability (1975) 1868, see also Chem. Abstr., 85 (1976) 34538.
15 A. Granzo, Acc. Chem. Res., 11 (1978) 177.
16 J.G. Dupont and C.W. Allen, Macromolecules, 12 (1979) 169.
17 R.A. Shaw, B.W. Fitzsimmons and B.C. Smith, Chem. Rev., 62 (1962) 247.
18 R. Keat and R.A. Shaw, Chemical Society Specialist Reports on Organophosphorus Chemistry, 1 (1969) 214.
19 I. Haiduc, The Chemistry of Inorganic Ring Systems, Part 2, Wiley, New York, 1970, p. 624.
20 R. Keat and R.A. Shaw, in G.M. Kosolapoff and L. Maier (Eds.), Organic Phosphorus Compounds, Vol. 6, Wiley, New York, 1973, p. 833.
21 J. Liebig and F. Wohler, Ann., 11 (1834) 139.
22 N.H. Stokes, Am. Chem. J., 17 (1895) 275.
23 L.G. Lund, N.L. Paddock, J.E. Proctor and H.T. Searle, J. Chem. Soc., (1960) 2542.
24 J. Emsley and P.B. Udy, J. Chem. Soc. A, (1970) 3025.
25 I.T. Gilson and H.H. Sisler, Inorg. Chem., 4 (1965) 273.
26 R.A. Shaw and E.H.M. Ibrahim, Angew. Chem. Int. Ed. Engl., 6 (1967) 556.
27 R.A. Shaw and F.B.G. Wells, Chem. Ind. (London), (1960) 1189.
28 K.G. Acock, R.A. Shaw and F.B.G. Wells, J. Chem. Soc., (1964) 121.
29 G.T. McBee, K. Okuhara and C.T. Morton, Inorg. Chem., 4 (1965) 1672.
30 M. Biddlestone and R.A. Shaw, J. Chem. Soc. A, (1969) 178.
31 M. Biddlestone and R.A. Shaw, J. Chem. Soc., Dalton Trans., (1973) 2740.
32 R.A. Shaw, Pure Appl. Chem., 44 (1975) 317.
33 M.I. Davis and J.W. Paul, Acta Crystallogr. Suppl., 25A (1969) 5116.
34 R. Olthof, T. Michelsen and A. Vos., Acta Crystallogr., 19 (1965) 596.
35 G.B. Ansell and G.J. Bullen, J. Chem. Soc. A, (1968) 3026.

36 I.C. Hisatsune, Spectrochim. Acta, Part A, 21 (1965) 1899.
37 T.R. Manley and D.A. Williams, Spectrochim. Acta, Part A, 23 (1967) 149.
38 N.V. Mani, F.R. Ahmed and W.H. Barnes, Acta Crystallogr., 19 (1965) 693; 21 (1966) 375.
39 C.D. Schmulbach and J. Derderian, Inorg. Nucl. Chem., 25 (1963) 1395.
40 M.B. Sayed, M.E. Kassem and I.M. Al-Emadi, Thermochim. Acta, 188 (1991) 143.
41 R.H. Boyd and L. Kesner, J. Am. Chem. Soc., 99 (1977) 4248.
42 J.P. Huvenne, G. Vergoten and P. Legrand, J. Mol. Struct., 63 (1980) 47.
43 P.C. Painter, J. Zarian and M.M. Coleman, Appl. Spectrosc., 63 (1982) 265.
44 M. Manfait, A.J.P. Alix, J.F. Labarre and F. Sourries, J. Raman Spectrosc., 12 (1982) 212.
45 L.C. Thomas, Interpretation of the Infrared Spectra of Organophosphorus Compounds, Heyden, London, 1974.
46 L.J. Bellamy, The Infrard Spectra of Complex Molecules, Chapman and Hall, London, 1975.
47 B. Lakatos, A. Hesz, Z. Vetessy and G. Harvath, Acta Chim. Acad. Sci. Hung., 66 (1969) 309.
48 A.J. Wagner and T. Moeller, J. Inorg. Nucl. Chem., 33 (1971) 1307.
49 D.S. Gaunt and C. Domb. J. Phys. C, 2(I) (1988) 1038.
50 M.F. Sykes, J.L. Martin and D.L. Hunter, Proc. Phys. Soc., 91 (1967) 671.
51 G.H. Meissner and H. Hais, Acta Phys. Austriaca Suppl., 18 (1977) 567.